GEOMORPHOMETRY 2020 PERUGIA, ITALY JUNE 22 - 26 2020

Detecting paleosurface remnants on open access digital elevation models

Bernadett Dobre, István Péter Kovács, Titusz Bugya
Doctoral School of Earth Sciences
University of Pécs
Ifjúság street 6, 7624 Pécs, Hungary
§berneeg@gamma.ttk.pte.hu

Abstract—**Using different openly accessible digital elevation models to classify terrain forms are applied broadly in geomorphometry research. But to use those DEMs properly we must know their capabilities in altering environments. Throughout our research we give a brief overview about the applicability of the openly accessible, 30 meter pixel sizing DEMs in a semi-arid study area. While examining a wide range of digital elevation models (DEMs) we are able to add our novel experiences to widen the current knowledge of DEM relevancies. In our case study we investigate different elevation models with GIS tools and commonly adopted statistics in order to evaluate the possibility to detect peak forms as possible paleosurface remnants. Our research outcome can benefit other related geomorphometric analysis and gives a new approach for paleosurface detection.**

I. Introduction

The possibility of analysing a wide range of open access global or quasi-global digital elevation models gives an outstanding possibility for several research areas such as geomorphology, hydrology and further associated geosciences. Using semi-automated surface recognition on these DEMs we have an opportunity to observe and classify numerous geomorphological forms and features [1, 2]. Our aim was to detect paleosurface remnants and through qualitative and quantitative evaluation find the most appropriate DEM regarding the above mentioned purpose.

1.1. Theoretical background

Due to the recurrent quaternary climate changes the landscape continuously formed related to changing presence of erosion and accumulation. As a result of these recurrent processes various surface remnant had been reserved in altering forms. Usually, older surface remnants can be found as noticeable peaks and summits [3]. The ability of detecting peaks and summits can lead to a more detailed paleogeographical researches.

1.2. Study area

Our study area is located in the the Desatoya Mountains along the border of Churchill and Lander counties in Nevada as a part of the Great Basin. The Great Basin is a semi-arid to arid region, where our study area has an average annual precipitation approx. 250-360 mm/yr, which the majority is falling as snow in the winter months [4].

The landscape of the research area is a mountainous region with steep slopes and valleys and alluvial plains.

1.3. Examined DEMs

In our study we tested four different digital elevation models. The first is a 30 meter resolution DEM, which was derived from open access Lidar points with 6.21 pts/m^2 point density for 61 km^2 area [5]. This model was also used as a validation for the other observed DEMs. We used three different global models to examine the study area: TanDEM-X with 30 meter resolution, SRTM1 v3.0 and ASTER GDEM v3.0. The TanDEM-X dataset was created using X-band SAR instruments and released by the German Aerospace Center (DLR) in 2016 [6]. The other studied interferometric DEM was the SRTM1 model imagined with C-band SAR, released by the collaboration of NASA, NGA, ASI and DLR in 2015 [7, 8]. Finally, we examined the latest version of ASTER GDEM photogrammetric model created by the METI and NASA and released at 2016 [9, 10].

II. Methods

Firstly, the above mentioned Lidar point cloud was downloaded, then Lidar data points we interpolated for a 1 and a 30 meter resolution reference DEM, using regular spline tension interpolation method with the GRASS GIS's default parameters. Descriptive and error statistics for each model were also calculated. The r.geomorphon GRASS module has been run [11], where the core size reflects to the sizes of the searched remnants. Using the module's outcomes, we created histograms to explore possible absence of the paleosurface groups. As a qualitative evaluation we edited maps and surface profiles to aid proper visualization.

2.1. Applied softwares

Throughout the research, GIS data processing was performed in GRASS GIS 7.6.1. [12], while for visualization we both used QGIS 3.4.6. and GRASS GIS 7.6.1. softwares. In order to reference the TanDEM-X heights to the EGM96 geoid we run F477 program provided by NGA [13]. The implementation and presentation of the statistical calculation were carried out in RStudio version 1.2.5033.

Bernadett Dobre, Istvín Pter Kovícs and Titusz Bugya (2020) Detecting paleosurfaces on open access DEMs in semi-arid study area: in Massimiliano Alvioli, Ivan Marchesini, Laura Melelli & Peter Guth, eds., Proceedings of the Geomorphometry 2020 Conference, doi:10.30437/GEOMORPHOMETRY2020_37.

2.2. Descriptive statistics and error measures

To evaluate the vertical accuracy of the DEMs, we created Dem of Differences (DoD) for each of the models and also calculated the following error metrics: RMSE, MAE (1), SD (2) and R^2 [14, 2, 1]. Throughout the calculations the reference DEM was the 30 meter Lidar model.

$$MAE = \frac{1}{n}\sum_{j=1}^{n}|y_j - \hat{y}_j| \quad (1)$$

$$SD = \sqrt{\frac{\sum|x - \bar{x}|^2}{n}} \quad (2)$$

2.3. Semi-automated recognition process

The detection of the paleosurface remnants *r.geomorphon* GRASS GIS module was evaluated [11, 15], which contains ten different surface feature categories. Knowing that our paleosurface interpretation is related to peak/summit forms, we used the summits category. Firstly we used *r.mapcalc* to select the summit category from the r.geomorphon output. Later the *r.thin modul was used* to "skeletonize" the output raster map. Following that we used *r.to.vect* to vectorize the selected areas which were transformed to points with the *v.to.point* function. Finally, we added a new column to the attribute table and refreshed it with the elevation data using *v.what.rast* module. The output text file contains the x and y coordinates and the elevation, therefore it was appropriate to create histograms with various core sizes in order to explore the presence of the different paleosurfaces. Those histograms were clasterized and summarized in the Fig. 1 and Fig. 2.

III. Results and Conclusions

Examining the research outcome, seven distinct groups of possible paleosurfaces were detected. Five of them stand out sharply, while the rest of them can be interpreted as sub-surfaces also. The surfaces related to lower elevation are clearly separated, however the middle of the histogram is quite variant (Fig. 1.). The summits occurring at higher elevations are clearly separable at the same time due to its larger extents and also more eroded (Fig. 2.).

While examining the statistical parameters on Table 1., the TanDEM-X model was proved to be the most accurate considering RMSE, MAE and also R^2 value. The SRTM1 model stands close to the TDX, which could be a result of the same imaging system. The ASTER GDEM came out as the least precise of all.

On Fig. 3. A, the ASTER GDEM showed less precise on lower elevation with numerous misdetection, moreover the number of intersection proved lower compared to any other DEM. The SRTM1 (Fig. 3. B) model had almost twice as much many intersecting point as the ASTER DEM.

The TanDEM-X model (Fig. 3. C) gave the most impressive match with the Lidar model, practically twice as many as the SRTM1.

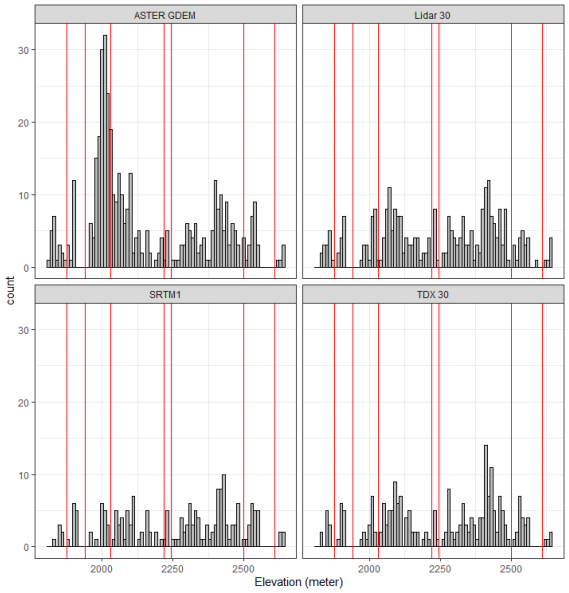

Figure 1. Histogram of each DEM with possible paleosurface remnants (dashed red lines)

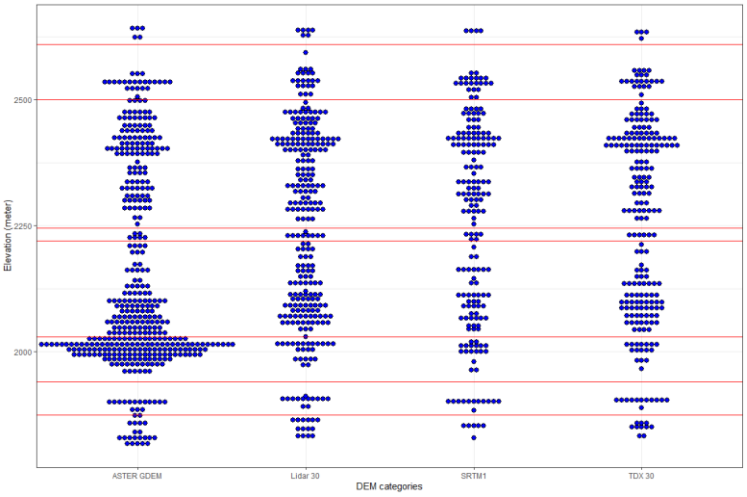

Figure 2. The dot plot of each DEM with the possible paleosurfaces (solid red lines)

Data	Imaging system	Wavelength	Pixel spacing	RMSE	MAE	R^2
SRTM1	SAR-C	5,66 cm	30	4,966	3,599	0,9996
ASTER	OPTICAL	0,52–10,95 µm	30	9,581	6,979	0,9985
TDX30	SAR-X	3,1 cm	30	3,381	2,415	0,9998
Lidar	OPTICAL	1064 nm	30	-	-	1

Table 1. Basic parameters and measure statistical errors of each DEM.

The remnant detection was successful on all of the models, while the TanDEM-X gave the most accurate outcome compared to the Lidar DEM, which was expected knowing its resolution. SRTM1 model proved also accurate enough and quite similar to the TanDEM-X, mostly also by the reason of the similar data acquisition techniques used for DEM creation. On Fig. 3. A, the ASTER GDEM showed less precise on lower elevation with numerous misdetection, moreover the number of intersection proved lower compared to any other DEM. The SRTM1 (Fig. 3. B) model had almost twice as much many intersecting point as the ASTER DEM. The TanDEM-X model (Fig. 3. C) gave the most impressive match with the Lidar model, practically twice as many as the SRTM1.

High number of the remnants can be interpreted as both fluvial and lacustrine erosion, furthermore the frequent tectonics [4] could leave a mark too, but this can only be the conclusion of a later research.

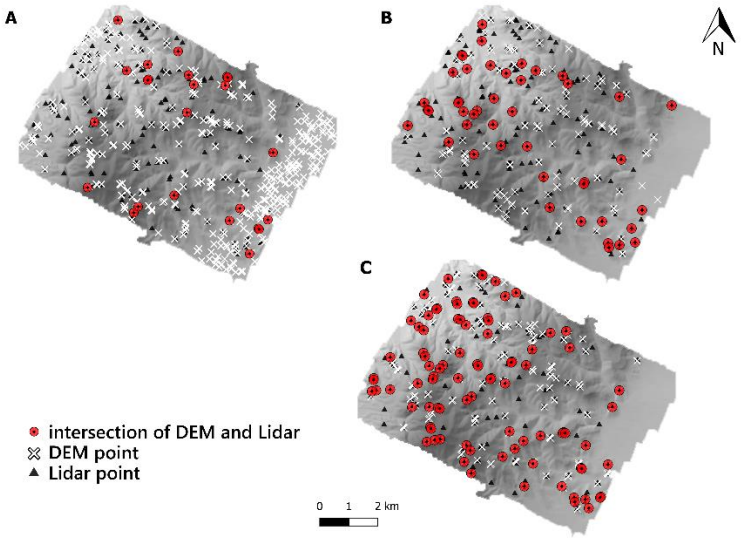

Figure 3. Intersection of DEM points and Lidar points, where A=ASTER GDEM, B=SRTM1, C=TDX

REFERENCES

[1] Sandip Mukherjee, P.K. Joshi, Samadrita Mukherjee, Aniruddha Ghosh, R.D. Garg, Anirban Mukhopadhyay 2013. Evaluation of vertical accuracy of open source Digital Elevation Model (DEM). International Journal of Applied Earth Observation and Geoinformation, 21, 205-217.

[2] Józsa, E., Fábián, S. Á., & Kovács, M. 2014. An evaluation of EU-DEM in comparison with ASTER GDEM, SRTM and contour-based DEMs over the Eastern Mecsek Mountains. Hungarian Geographical Bulletin, 63(4), 401–423.

[3] Bugya, T. 2009. Identification of Quaternary fluvial terraces using borehole data and digital elevation models. Zeitschrift Für Geomorphologie, Supplementary Issues, 53(2), 113–121.

[4] Chambers, Jeanne C.; Miller, Jerry R., eds. 2011. Geomorphology, hydrology, and ecology of Great Basin meadow complexes—implications for management and restoration. Gen. Tech. Rep. RMRS-GTR-258. Fort Collins, CO: U.S. Department of Agriculture, Forest Service, Rocky Mountain Research Station. 125 p.

[5] http://opentopo.sdsc.edu/datasetMetadata?otCollectionID=OT.102016.26911.1

[6] Grohmann, C. H. 2018. Evaluation of TanDEM-X DEMs on selected Brazilian sites: Comparison with SRTM, ASTER GDEM and ALOS AW3D30. Remote Sensing of Environment, 212, 121–133.

[7] Farr, T. G., Rosen, P. A., Caro, E., Crippen, R. E., Duren, R., Hensley, S., … Alsdorf, D. E. 2007. The Shuttle Radar Topography Mission. Reviews of Geophysics, 45(RG2004), 1–33.

[8] Guth, P. L. 2010. Geomorphometric Comparison of ASTER GDEM and SRTM. ISPRS Archives – Geospatial Data and Geovisualization: Environment, Security, and Society, 1–10. Orland

[9] Abrams, M. 2016. ASTER global DEM version 3, and new ASTER Water Body Dataset. ISPRS Annals of Photogrammetry, Remote Sensing and Spatial Information Sciences, 107–110. Prague: Copernicus Publications.

[10] ASTER Global Digital Elevation Map Announcement. 2011. Retrieved March 11, 2019, from https://asterweb.jpl.nasa.gov/gdem.asp

[11] Stepinski, T. F., & Jasiewicz, J. 2011. Geomorphons - a new approach to classification of landforms. In T. Hengl, I. S. Evans, J. P. Wilson, & M. Gould (Eds.), Proceedings of Geomorphometry 2011 pp. 109–112. Redlands: International Society for Geomorphometry.

[12] Hofierka, J., Mitasova, H., & Neteler, M. 2009. Geomorphometry in GRASS GIS. In T. Hengl & H. I. Reuter (Eds.), Geomorphometry: Concepts, Software, Applications. Developments in Soil Science, vol. 33 (pp. 387–410). Amsterdam: Elsevier.

[13] https://earthinfo.nga.mil/GandG/wgs84/gravitymod/egm96egm96.html

[14] Ismail Elkhrachy 2018. Vertical accuracy assessment for SRTM and ASTER Digital Elevation Models: A case study of Najran city, Saudi Arabia. Ain Shams Engineering Journal, 9, 1807-1817.

[15] Michal Veselský, Peter Bandura, Libor Burian, Tatiana Harciníková, and Pavel Bella 2015. Semi-automated recognition of planation surfaces and other flat landforms: a case study from the Aggtelek Karst, Hungary. Open Geosciences, 1, 799-811.